Synthesis and Charge/Discharge Properties of Polyacetylenes Carrying 2,2,6,6-Tetramethyl-1-piperidinoxy Radicals

Jinqing Qu,[a] Toru Katsumata,[a] Masaharu Satoh,[b] Jun Wada,[c] Jun Igarashi,[d] Kenji Mizoguchi,[d] and Toshio Masuda*[a]

Abstract: The 2,2,6,6-tetramethyl-1-piperidinoxy (TEMPO)-containing acetylenic monomers HC≡CC$_6$H$_3$-p,m-(CONH-4-TEMPO)$_2$ (**1**), HC≡CC$_6$H$_3$-p,m-(COO-4-TEMPO)$_2$ (**2**), (S,S,S,S)-HC≡CC$_6$H$_3$-p,m-[CO-NHCH{COO-(4-TEMPO)}CH$_2$COO-(4-TEMPO)]$_2$ (**3**), (S,S)-HC≡CC$_6$H$_4$CO-NHCH{COO-(4-TEMPO)}CH$_2$COO-(4-TEMPO) (**4**), HC≡CC$_6$H$_4$-p-OCO-4-TEMPO (**5**), HC≡CCH$_2$C(CH$_3$)(CH$_2$OCO-4-TEMPO)$_2$ (**6**), HC≡CCH$_2$NHCO-4-TEMPO (**7**), and HC≡CCH$_2$OCO-4-TEMPO (**8**) were polymerized to afford novel polymers containing the TEMPO radical at high densities. Monomers **1**, **3–6**, and **8** provided polymers with average molecular weights of 10 000–136 500 in 62–99 % yield in the presence of a rhodium catalyst, whereas monomers **2** and **7** gave insoluble polymers in 100 % yield. The formed polymers were thermally stable up to approximately 274 °C according to thermogravimetric analysis (TGA). All the TEMPO-containing polymers demonstrated reversible charge/discharge processes, whose discharge capacities were 21.3–108 A h kg^{-1}. In particular, the capacity of poly(**1**)-, poly(**4**)-, and poly(**5**)-based cells reached 108, 96.3, and 89.3 A h kg^{-1}, respectively, which practically coincided with their theoretical values.

Keywords: batteries · charge/discharge properties · electrochemistry · organic radicals · polyacetylenes · polymers

Introduction

Stable organic radicals are widely used as spin labels[1] for monitoring the functions of biomolecules and as spin traps or radical scavengers[2] of organic materials and biological systems. Polymers that carry stable organic radicals have been intensively studied as subjects of electron spin resonance[3] and molecular motion[4] and frequently employed as functional materials, such as polymeric stabilizers,[5] oxidants of alcohols,[6] and spin- and charge-storage materials.[7] Among these applications, polymers with π-conjugated radicals,[8] especially polyacetylenes containing stable radicals,[9] have been extensively studied in the search for organic ferromagnetic materials.

2,2,6,6-Tetramethyl-1-piperidinyloxy (TEMPO) and its derivatives are well-known stable nitroxy radicals[10] and have found application in a variety of fields, such as spin labels in the study of conformation and structural mobility of biological systems,[11] scavengers of unstable radical species,[12] and oxidizing agents.[13] The TEMPO radical is a typical oxygen-centered radical with a resonance structure in which an odd electron is delocalized onto a nitrogen atom, thus contributing to its high stability. The TEMPO radical displays two redox couples, namely, oxidation to a cation and reduction to an anion: it can be oxidized to form the corresponding oxoammonium cation, the oxidation process of the radical is reversible and leads to p-type doping of the radical material, and it can also be reduced to the aminoxy anion, thus resulting in n-type doping of the material. By using the oxidation process to the cation, TEMPO-carrying polymers can be applied to cathode-active materials in secondary batteries, and

[a] J. Qu, T. Katsumata, Prof. Dr. T. Masuda
Department of Polymer Chemistry
Graduate School of Engineering, Kyoto University
Katsura Campus, Kyoto 615-8510 (Japan)
Fax: (+81) 75-383-2590
E-mail: masuda@adv.polym.kyoto-u.ac.jp

[b] M. Satoh
Fundamental and Environmental Research Laboratories
NEC Corporation, 34, Miyukigaoka
Tsukuba, Ibaraki 305-8501 (Japan)

[c] J. Wada
Corporate Planning Department
Nippon Kasei Chemical Co., Ltd.
1-8-8 Shinkawa, Chuoku, Tokyo 104-0033 (Japan)

[d] J. Igarashi, Prof. K. Mizoguchi
Department of Physics
Tokyo Metropolitan University
Hachi-oji, Tokyo 192-0397 (Japan)

such batteries can be called organic radical batteries. As compared to the currently popular lithium-based batteries, organic radical batteries feature high-speed charging and discharging.

Poly(2,2,6,6-tetramethylpiperidinyloxy methacrylate) (PTMA) was examined as a material for the first-generation organic radical batteries, which could be rapidly charged and had a high power density.[14] Thus far, polymers carrying nitroxy free radicals, such as PTMA, are usually synthesized by an indirect method, namely, the synthesis of precursor polymers with the corresponding amino group, followed by oxidation to afford polymers containing stable radicals.[15] The indirect route is adopted as a result of the inability of radical-bearing monomers to undergo radical polymerization. However, this method is often accompanied by incomplete oxidation, thus resulting in less than quantitative incorporation of the radical into the polymer.[16] As a consequence, PTMA did not have the quantitative amount of radicals but approximately 70% against the theoretical value, and the batteries using this polymer showed an average discharge voltage of 3.5 V and a discharge capacity of 77 A h kg^{-1} (70% of the theoretical value). Noting that transition-metal catalysts may polymerize radical-bearing monomers, we recently investigated the preparation and charge/discharge properties of several polyacetylenes and polynorbornenes containing TEMPO groups as a preliminary study and revealed that the discharge capacity of the cell fabricated with poly[norbornene-2,3-*endo,exo*-(COO-4-TEMPO)$_2$] reached the theoretical value (109 A h kg^{-1}) expected for the molecular structure.[17] More recently, Nishide and co-workers reported that poly[4-(*N-tert*-butyl-*N*-oxylamino)styrene], poly[3,5-di(*N-tert*-butyl-*N*-oxylamino)styrene], and poly[4-(*N-tert*-butyl-*N*-oxylamino)-3-trifluoromethylstyrene] possessed radical densities of 1.82–4.27 × 10^{21} unpaired electrons g^{-1}, and these polymers might be applicable as electrode-active materials with a high charge/discharge capacities.[18]

Substituted polyacetylenes exhibit unique properties, such as chromism, semiconductivity, paramagnetism, high gas permeability, helix formation, and nonlinear optical propert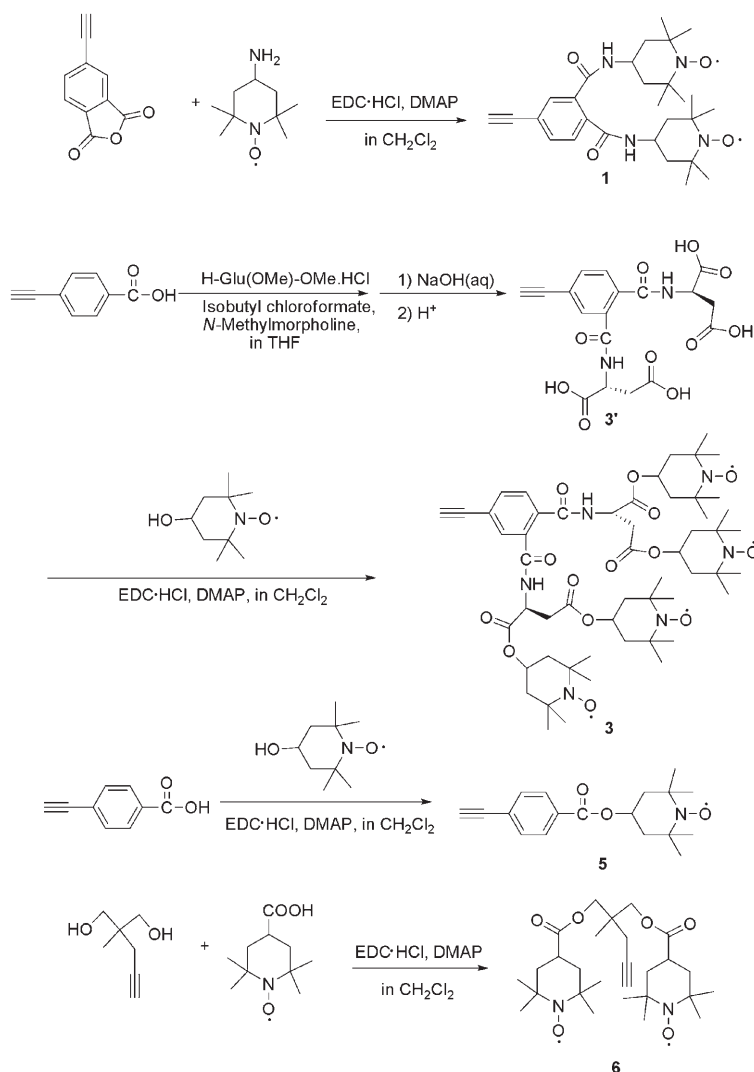ies.[19] The introduction of TEMPO moieties into polyacetylene may lead to new functional materials based on the synergistic effect of stable organic radicals and a main chain of conjugated polyacetylene units. Herein, we discuss the synthesis of TEMPO-carrying polyacetylenes by direct polymerization of TEMPO-containing acetylenes (Scheme 1) with a rhodium-based transition-metal catalyst and report on fundamental properties, such as charge/discharge characteristics of the formed polymers as cathode-active materials in an organic-radical battery.

Results and Discussion

Monomer synthesis: Scheme 2 illustrates the synthetic routes to monomers **1–6**. Acetylene ester and amide monomers **1** and **2** were synthesized by the reaction of 4-ethynylphthalic anhydride with the hydroxy or amino group of TEMPO derivatives. Monomers **3** and **4** were synthesized by the reaction of 4-hydroxy-TEMPO with **3'** ($M_w = 420.33$) for **3** and *N*-(4-ethynyl benzoyl)-L-aspartic acid for **4**, which were prepared from 4-ethynylphthalic anhydride and 4-ethynylbenzoic acid reaction with L-H-Glu(OMe)-OMe·HCl,
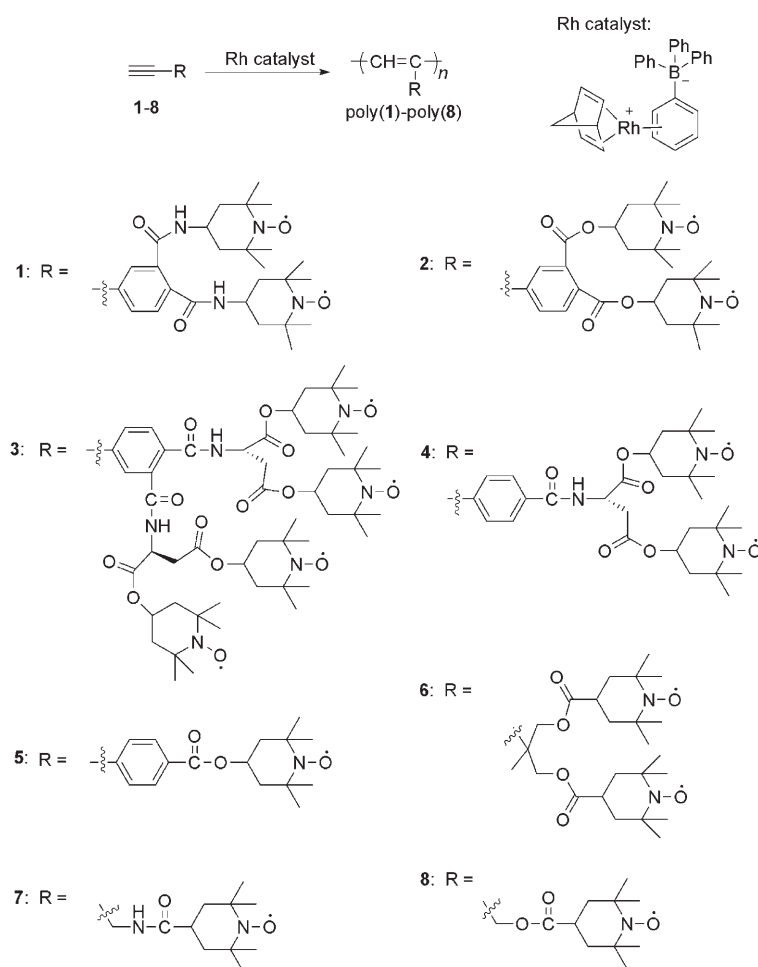
Scheme 1. Synthesis of TEMPO-containing polyacetylenes by direct polymerization of TEMPO-containing acetylenes.

Scheme 2. Synthesis of acetylene monomers **1**, **3**, **5**, and **6**.

and 7 in Table 1). However, poly(**2**), which was obtained at a lower monomer concentration ($[M]_0 = 0.10$ M), was soluble in organic solvents, although the polymer yield was rather low (38%). On the other hand, **1**, **3**–**6**, and **8** gave solvent-soluble polymers with number-average molecular weights of 10000—136500 in 62–99% yield (runs 1, 3–6, and 8 in Table 1). All the polymers were orange, which is attributable to the TEMPO side chains and/or the conjugated main chain.

Structure of the polymers: Poly(**1**)–poly(**8**) did not exhibit IR absorptions at about 3300 and 2120 cm^{-1} that arise from the stretching vibrations of H-C≡ and -C≡C-, respectively, thus indicating that ordinary acetylene polymerization took place. The IR spectra of all the polymers showed a strong absorption maximum at 1364 cm^{-1} assignable to the nitroxy radical, thus implying that the TEMPO moiety is present in the polymers.

Properties of the polymers: Poly(**1**), poly(**3**)–poly(**5**), and poly(**8**) were soluble in relative-

then by removing the methyl group of products. Monomer **5** was prepared by condensation of the hydroxy group of 4-hydroxy-TEMPO with the carboxy group of 4-ethynylbenzoic acid. Monomer **6** was synthesized by the reaction of 1-pentyne-4,4-dimethanol with two equivalents of 4-carboxy-TEMPO. Monomers **1**–**6** were purified by column chromatography on silica gel eluted with ethyl acetate/*n*-hexane (1:4 v/v). As a result of the presence of free radicals, it was impossible to measure the NMR spectra of the monomers. The structures of the monomers were confirmed by IR spectroscopic and elemental analysis.

Polymer synthesis: The polymerization of acetylene monomers **1**–**8** was carried out using [Rh$^+$(nbd){η^6-C$_6$H$_5$B$^-$-(C$_6$H$_5$)$_3$}] (nbd = norbornadiene) as a catalyst at 30°C for 24 h (Table 1). Polymeric compounds were obtained quantitatively by the polymerization of **2** and **7**, but these polymers were insoluble in common organic solvents, including THF, CHCl$_3$, and *N,N*-dimethylformamide (DMF; runs 2

Table 1. Polymerization of acetylenic monomers **1**–**8** with [Rh$^+$(nbd){η^6-C$_6$H$_5$B$^-$(C$_6$H$_5$)$_3$}].

Run	Monomer	Polymer		
		yield [%][a]	M_n[b]	M_w/M_n[e]
1[b]	**1**	99	108900	4.75
2[b]	**2**	100	—[f]	—[f]
3[c]	**3**	95	125700	4.43
4[c]	**4**	99	83800	3.39
5[c]	**5**	97	136500	4.68
6[d]	**6**	62	10000	1.36
7[d]	**7**	100	—[f]	—[f]
8[d]	**8**	66	47000	2.01

[a] MeOH-insoluble part. [b] Determined by GPC (THF, polystyrene calibration). [c] In THF, 24 h, 30°C; $[M]_0 = 0.50$ M, [Rh] = 10 mM. [d] In THF, 24 h, 30°C; $[M]_0 = 0.25$ M, [Rh] = 2.5 mM. [e] In CHCl$_3$, 24 h, 30°C; $[M]_0 = 0.25$ M, [Rh] = 2.5 mM. [f] Insoluble as a result of gelation.

ly nonpolar organic solvents, including toluene, CHCl$_3$, CH$_2$Cl$_2$, and THF, but were insoluble in *n*-hexane, methanol, and diethyl ether. Poly(**6**) was soluble in CHCl$_3$ and THF,

partly soluble in toluene and CH_2Cl_2, and insoluble in *n*-hexane, methanol, and diethyl ether. Polymers poly(**2**) and poly(**7**) were insoluble in common organic solvents. Figure 1 illustrates the thermogravimetric analysis (TGA) traces of the present polymers. The onset temperatures of weight loss of poly(**1**)–poly(**8**) were all around 220–274 °C in air. All of the polymers containing TEMPO decomposed in similar fashions. All of the present polymers completely decomposed when the temperature was raised above 650 °C.
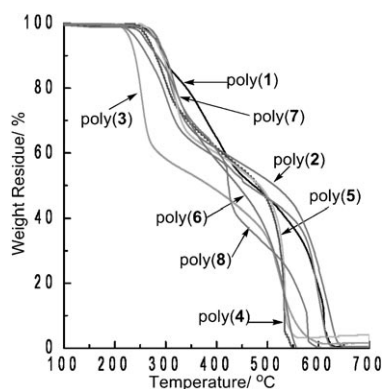

Figure 1. TGA curves of poly(**1**)–poly(**8**) measured at a heating rate of 10 °C min^{-1} in air.

The cyclic voltammetry (CV) curves of poly(**1**) and poly(**4**) are shown in Figure 2. Reversible oxidation and reduction based on the TEMPO radical are observed for all the polymers. Poly(**1**) exhibits an oxidation potential peak at 0.507 V versus Ag/Ag$^+$ and a reduction potential peak at 0.459 V versus Ag/Ag$^+$ at a sweep rate of 0.01 V s^{-1}, whereas poly(**4**) shows corresponding peaks at 0.504 and 0.431 V, respectively. It is noted that the distances between the oxidation and reduction potential peaks of poly(**1**) and poly(**4**) are 0.048 and 0.073 V, respectively, which are by far smaller than those of other electroactive organic materials such as PTMA (ca. 0.146 V).[14] The small gaps between the reduction and oxidation peaks generally imply large electrode reaction rates of the polymers, which suggests that these polymers will exert high power rates in the charge/discharge processes of battery under the constant battery process conditions. The oxidation and reduction peaks of poly(**1**) and poly(**4**) scarcely changed after five CV scans, thus indicating that they were quite stable electrochemically.

Figure 3 shows the electron spin resonance (ESR) spectrum of poly(**1**) and poly(**2**). The ESR spectra of poly(**1**) and poly(**2**) exhibited sharp singlet signals based on the TEMPO moiety at $g = 2.0070$ and 2.0064 respectively, which are close to $g = 2.0055$ for the 4-hydroxy-2,2,6,6-tetramethyl-piperidine-1-oxyl (TEMPOL) crystal; the small enhancement is probably a result of the effect of the polymer backbone. The spin concentration of poly(**1**) and poly(**2**) were tested up to 2.53×10^{21} and 2.41×10^{21} spins g^{-1}, respectively, and were much larger than that of PTMA; hence, the local-spin concentrations within the macromolecular domains of

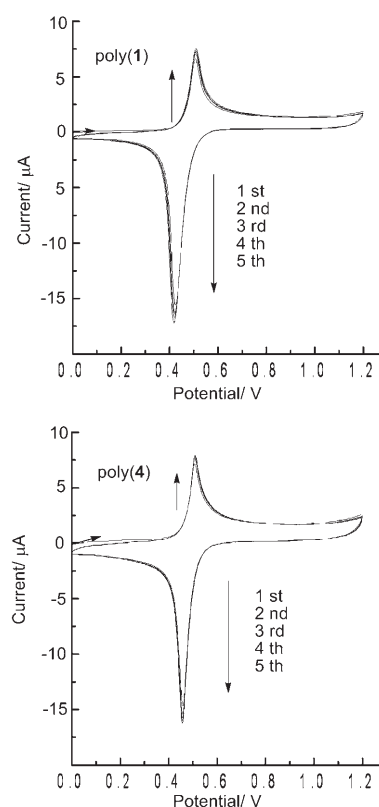Figure 2. Cyclic voltammograms of poly(**1**) and poly(**4**) measured at a scan rate of 0.01 V s^{-1} versus Ag/Ag$^+$ in solution with TBAP.
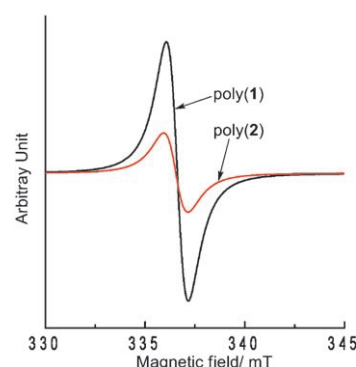

Figure 3. ESR spectrum of poly(**1**) and poly(**2**) measured in the powder state.

poly(**1**) and poly(**2**) are higher than that of PTMA. The ESR spectra of other polymers were similar to that of poly(**1**). Further, we determined the spin concentrations and magnetic properties of poly(**1**), poly(**2**), and poly(**7**) precisely (Table 2). As seen from Table 2, poly(**1**), poly(**2**), and poly(**7**) possess approximately quantitative amounts of free radicals, that is, relatively close to 1 in poly(**7**) and around 2 in poly(**1**) and poly(**2**) per repeating unit. Both the Curie–Weiss temperature Θ and the frequency dependence of the ESR line width are consistent with the 1D magnetic interaction between the TEMPO radicals attached to the polymer backbone. The Θ value of the polymers with the 1D chain

Table 2. Magnetic properties of polymers.

Polymer	Number of spins per monomer unit	Curie–Weiss temperature Θ [K]	ESR g-factor	ESR line width [G]	
				≈ 50 MHz	≈ 9400 MHz
Poly(**1**)	2.03 ± 0.10	1.9	2.0070	13.9	9.9
Poly(**2**)	1.96 ± 0.10	1.8	2.0064	12.6	8.9
Poly(**7**)	0.83 ± 0.05	1.5	2.0064	13.0	8.6

of TEMPO radicals should be smaller than about 7 K of the TEMPOL crystal, in which the 3D magnetic interaction dominates the Θ value. The ESR line widths vary with the ESR frequency in the 1D electronic systems[23] (Table 2).

Figure 4 exhibits the charge/discharge curves of the cells fabricated using poly(**1**)-poly(**8**) measured at a constant current density of 0.030–0.096 A g^{-1} in the voltage range of 2.5–4.2 V. During the charge process of poly(**1**), the voltage sharply increased from 3.0 to 3.5 V with a cell capacity in the range 0–10 A h kg^{-1}, followed by a highly steady voltage plateau at about 3.5–3.7 V up to a cell capacity of 95 A h kg^{-1}, and the voltage finally increased to a top cut-off voltage of 4.2 V. Similarly, during the discharge process of poly(**1**), the voltage quickly decreased from 4.2 to 3.7 V within a cell capacity of 0–8 A h kg^{-1}, followed by a steady voltage plateau at about 3.7–3.4 V until a capacity of up to 97 A h kg^{-1}, and the voltage then gradually decreased to a

bottom cut-off voltage at 2.5 V. The plateau voltages of the charge/discharge processes are in the range 3.4–3.7 V starting from approximately 3.6 V, which corresponds to the redox potential of the TEMPO radical. The charge/discharge processes of poly(**2**)–poly(**8**) behaved in a similar way to poly(**1**). Namely, all of the present polymers exhibit a clear voltage plateau at about 3.6 V in both the charge and discharge curves, thus indicating that the polymers can be used as cathode-active materials of a rechargeable battery.

It is reasonable to assume that the charge process at the cathode is the oxidation of the TEMPO units (**9**) in the polymers to an oxoammonium salt (**10**), and the discharge process is the opposite reaction, namely, the reduction of the salt (Scheme 3). Taking into account that one TEMPO
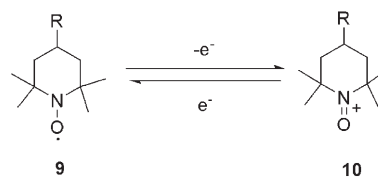
Scheme 3. Charge/discharge processes.

moiety provides one electron in this redox process, we can estimate the theoretical capacities of the cells based on poly(**1**)–poly(**8**) to be 89.3–113 A h kg^{-1} (Table 3). Evaluation of the values given at 2.5 V in Figure 3: the initial discharge capacities of the cells using poly(**1**)–poly(**8**) are determined to be 21.3–108 A h kg^{-1} per polymer weight at a current density of 0.030–0.096 A g^{-1}. The observed discharge capacities of poly(**1**), poly(**4**), and poly(**5**) were 108, 96.3, and 89.3 A h kg^{-1}, respectively, which agreed with the theoretical capacity. This result demonstrates that poly(**1**), poly(**4**), and poly(**5**) display high capacities, thus leading to a wide range of potential applications as power sources. On the other hand, the capacities of the cells based on poly(**2**)-, poly(**3**)-, and poly(**6**)–poly(**8**) remained 21.3, 62.3, 63.0, 80.5, and 66.0 A h kg^{-1}, respectively (Table 3), which are clearly
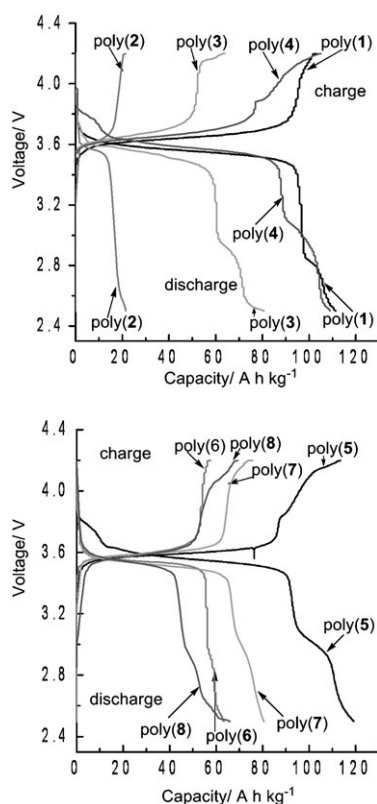
Figure 4. Charge/discharge curves of poly(**1**)–poly(**8**) at a current density of 0.030–0.096 A g^{-1} with a cell voltage of 2.5–4.2 V.

Table 3. Capacity data of poly(**1**)–poly(**8**)

Polymer	m/z[a]	Theoretical capacity [A h kg^{-1}][b]	Observed capacity [A h kg^{-1}][c]	Observed capacity/ theoretical capacity [%]
Poly(**1**)	248.3	108.0	108.0	100
Poly(**2**)	249.3	107.5	21.3	19.8
Poly(**3**)	252.3	106.2	62.3	58.7
Poly(**4**)	277.8	96.5	96.3	100
Poly(**5**)	300.2	89.3	89.3	100
Poly(**6**)	246.3	108.9	63.0	58.0
Poly(**7**)	227.3	113.0	80.5	71.2
Poly(**8**)	238.3	112.0	66.0	58.9

[a] The polymer mass required per exchangeable unit. [b] Theoretical capacity: specific charge calculated according to reference [26]. [c] Observed capacity: initial discharge capacity at a current density of 0.030–0.096 A g^{-1}, cut-off at 2.5 V.

lower than that of the poly(**1**)-based counterpart, although the theoretical capacities of the cells are all about 100 A h kg^{-1}. This behavior seems to be a result of the differences in both molecular scale structures (e.g., the spacial arrangement of the TEMPO radicals) and macroscopic aggregation states (e.g., the size and hardness of the polymer powders) but not in the spin concentration (because the spin concentrations of poly(**2**) and poly(**7**) are all quantitative).

Figure 5 depicts the charge/discharge curves of poly(**1**) and poly(**5**) observed at different current densities. The charge and discharge capacities gradually decreased with in-
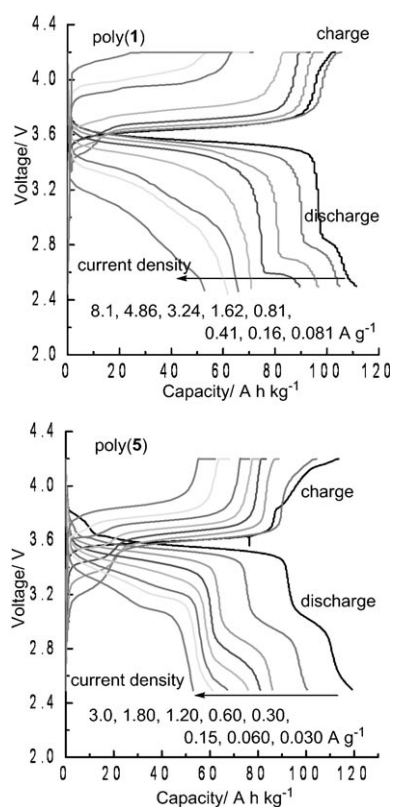

Figure 5. Charge/discharge curves of poly(**1**) and poly(**5**) at different currents with a cell voltage of 2.5–4.2 V.

creasing current densities. An effective capacity of approximately 53.0 A h kg^{-1} was attained at a current density of 8.10 A g^{-1} based on a cut-off voltage of 2.5 V for poly(**1**), which corresponds to 50 % of the discharge capacity at 0.081 A g^{-1} and indicates that the poly(**1**)-based cell displays excellent charge/discharge characteristics under the extremely large currents. The fabricated cell contains 1.23 mg of poly(**1**) as an electroactive material, and so the cell capacity of 108 A h kg^{-1} is calculated as 0.133 mA h. In this experiment, the current density of 8.1 A g^{-1} corresponds to 10 mA, which is capable of charging and discharging the cell within 0.0133 h (47.9 s). The poly(**5**)-based cell, in which the

discharge capacity at 3.0 A g^{-1} was above 50 A h kg^{-1}, exhibited a similar performance to that of poly(**1**).

Figure 6 depicts the relationship between capacity and the current densities of poly(**1**)–poly(**8**). The large capacity of poly(**4**) was fairly well maintained even though the current
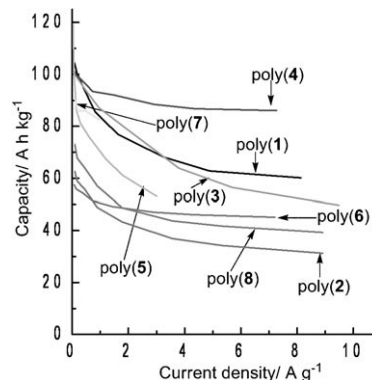

Figure 6. Dependence of capacity on current densities in poly(**1**)–poly(**8**).

densities were increased to 7.3 A g^{-1}. On the other hand, the capacity of the other polymers decreased more with increasing current densities. Thus, the largest capacity is available in the discharge of poly(**4**) among the present polymers irrespective of the current densities. Poly(**1**), poly(**3**), and poly(**5**) displayed pretty large capacities even though high current densities up to 3–9 A g^{-1} were applied. On the other hand, poly(**2**) and poly(**6**)-poly(**8**) showed worse behavior.

Figure 7 illustrates the cycle performance of the poly(**1**)–poly(**6**)/Li cells, in which charging and discharging were repeated at a current density of 0.30–0.96 A g^{-1} (1 mA current per 1.04–2.72 mg) under the application of cell voltages of 2.5–4.2 V. The capacity of the cell using poly(**1**) was maintained at over 85 % after 100 cycles. Poly(**2**) exhibited a different cycle performance; namely, the increase in capacity was observed, which appears to arise from the increase in the contact surface between the electrode and the electro-
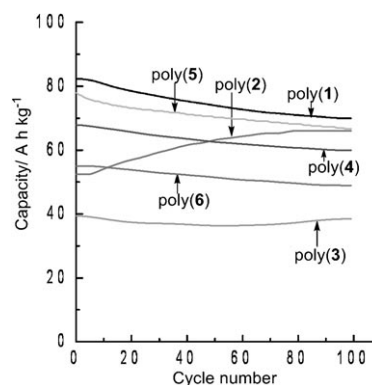

Figure 7. Dependence of capacity on cycle number in poly(**1**)–poly(**6**). Charging and discharging were repeated at a current density of 0.30–0.96 A g^{-1} with a cell voltage of 2.5–4.2 V.

lyte probably because of the swelling of the polymer during the charge/discharge process. The discharge capacity of poly(**3**) did not deteriorate even after 100 cycles. The lifecycles of cells based on poly(**4**)–poly(**6**) were similar to that of poly(**1**). It seems that the lifecycles of cells based on poly(**1**)–poly(**6**) are comparable to that of the reported PTMA system.[14]

Conclusion

Herein, we have synthesized a group of acetylenic monomers **1**–**8** containing TEMPO and polymerized them with a rhodium catalyst. Monomers **1**, **3**–**6**, and **8** provided polymers with number-average molecular weights of 10 000—108 900 in 62–99 % yield, while **2** and **7** gave insoluble polymers in 100 % yield. The separation of the oxidation and reduction potential peaks of these polymers in CV were by far smaller than those of other electroactive organic materials, which is indicative of a high power rate in the charge/discharge processes of the battery. The ESR spectrum of poly(**1**) and poly(**2**) exhibited a sharp singlet, and poly(**1**) and poly(**2**) possessed practically quantitative amounts of free radicals based on the TEMPO moiety, namely, around two spins per repeating unit. The capacity of cells based on poly(**1**)-, poly(**4**)-, and poly(**5**) reached 108, 96.3, and 89.3 A h kg^{-1}, respectively, corresponding to 100 % of their theoretical capacity value. The cells fabricated with poly(**1**)–poly(**6**) as cathodes demonstrated a promising cycle life, namely, the capacity hardly deteriorated even after 100 cycles. Charge-storage materials based on poly(**1**)–poly(**8**) can be applied to cathode-active materials in organic radical batteries, which show quick charging/discharging and high power density. Among the present polymers, poly(**4**) exhibited a high capacity up to 96.3 A h kg^{-1}, which did not decrease below 90 A h kg^{-1}, even at high current densities of up to 7.3 A g^{-1}, and the excellent performance was kept even after 100 cycles.

Experimental Section

Materials: Solvents used for polymerization were distilled before use according to standard procedures. 4-Carboxy-TEMPO (TCI), 4-hydroxy-TEMPO (TCI), L-Glutamic acid-α,γ-dimethyl ester hydrochloride (L-H-Glu(OMe)-OMe·HCl) (Watanabe Chemical Industries, Ltd), propargyl alcohol (Aldrich), propargylamine (Aldrich), N-(3-dimethylaminopropyl)-N′-ethylcarbodiimide hydrochloride (EDC·HCl; Eiweiss Chemical Corporation), 4-dimethylaminopyridine (DMAP; Wako) were purchased and used without further purification. 4-Carboxy-2,2,6,6-tetramethyl-1-piperidinoxy N-propargylamide,[17] 4-carboxy-2,2,6,6-tetramethyl-1-piperidinoxy propargyl ester,[17] 1-pentyne-4,4-dimethanol,[20] 4-ethynylbenzoic acid,[21] N-(4-ethynyl benzoyl)-L-aspartic acid methyl ester,[22] and [Rh$^+$(nbd){η^6-C$_6$H$_5$B$^-$(C$_6$H$_5$)$_3$}]][23] were synthesized according to previous reports.

Measurements: IR spectra were measured using a JASCO FT/IR-4100 spectrophotometer. Melting points (m.p.) were measured on a Yanaco micro melting-point apparatus. Elemental analysis was conducted at the Kyoto University Elemental Analysis Center. The number- and weight-average molecular weights (M_n and M_w, respectively) of polymers were

determined by gel-permeation chromatography (GPC) on a JASCO Gulliver system (PU-980, CO-965, RI-930, and UV-1570) equipped with Shodex columns KF805 L×3, using THF as the eluent at a flow rate of 1.0 mL min^{-1}, calibrated with polystyrene standards at 40 °C. Thermal gravimetric analysis (TGA) was carried out on a Perkin-Elmer TGA-7. ESR spectra were measured on a JEOL JES-FR30 type X-band (9.48 GHz) spectrometer. The precise number of free radicals was estimated with a Quantum Design MPMS susceptometer and a home-built low-frequency ESR–NMR apparatus operated at around 50 MHz, 4-hydroxy-TEMPO was the reference radical, and the samples were tested in the solid state.[24] Cyclic voltammograms were observed with an HCH Instruments ALS600 A-n electrochemical analyzer. The measurements were carried out with a modified indium tin oxide (ITO) substrate as the working electrode coupled with a Pt plate counter electrode and an Ag/AgCl reference electrode (Ag/AgCl/KCl (saturated)), using a solution of a polymer (1 mM) and tetrabutylammonium perchlorate (TBAP, 0.1 M) in CH$_2$Cl$_2$.

Monomer synthesis

4-Ethynylphthalic acid 1,2-di[4-(2,2,6,6-tetramethyl-1-piperidinyloxy)]-amide (1): 4-Amino-TEMPO (500 mg, 2.90 mmol) was added to a solution of EDC·HCl (581 mg, 3.04 mmol) and DMAP (37 mg, 0.30 mmol) in CH$_2$Cl$_2$ (30 mL) at room temperature. 4-Ethynylphthalic anhydride (250 mg, 1.46 mmol) was added to the solution, and the resulting mixture was stirred at room temperature overnight. The reaction mixture was washed with water (3×20 mL), and the organic layer was dried over anhydrous MgSO$_4$. After filtration, the solvent was removed by rotary evaporation to afford the crude product, which was purified by column chromatography on silica gel with a hexane/ethyl acetate (4:1, v/v) as the eluent. An orange–red solid was obtained in 64 % yield (921 mg). M.p. 204.0–205.0 °C; IR (KBr): $\tilde{v}$ = 3257 (H-C≡), 3068 (N−H), 2976, 2938, 2104 (C≡C), 1645 (C=O), 1561 (N−H), 1329, 1243, 1179, 847 cm^{-1}; elemental analysis calcd (%) for C$_{28}$H$_{40}$O$_4$N$_4$: C 67.71, H 8.12, N 11.28; found: C 67.50, H 8.39, N 11.50.

4-Ethynylphthalic acid 1,2-di[4-(2,2,6,6-tetramethyl-1-piperidinyloxy)] ester (2): Synthesized from 4-ethynylphthalic anhydride and 4-hydroxy-TEMPO (2 equiv) in a manner similar to **1**. The product was obtained as an orange-red solid in 80 % yield. M.p. 140.0–141.0 °C; IR (KBr): $\tilde{v}$ = 3224 (H-C≡), 2976, 2935, 2106 (C≡C), 1736 (C=O), 1714 (C=O), 1603, 1465, 1365, 1295 (C-O), 1193, 1133, 1069, 963, 789, 769, 564 cm^{-1}; elemental analysis calcd (%) for C$_{28}$H$_{38}$O$_6$N$_2$: C 67.45, H 7.68, N 5.62; found: C 67.30, H 7.59, N 5.50.

Compound 3′: (Scheme 2) Synthesized from 4-ethynylphthalic anhydride and L-H-Glu(OMe)-OMe·HCl (2 equiv) by removing the methyl group of products according to previous reports.[22] The product was obtained as a white solid in 34 % yield. ^{1}H NMR (400 MHz, CDCl$_3$, 25 °C, TMS): δ = 2.16 (q, 2H, J = 7.26 Hz, −2CHC*H$_2$*COOH), 2.47 (q, 2H, J = 7.26 Hz, −2CHC*H$_2$*COOH), 3.22 (s, 1H, ≡C*H*), 4.81 (q, 2H, J = 6.99 Hz, −2NHC*H*COOH), 7.54–7.80 (m, 3H, Ar), 8.11 (d, 2H, −2NH); ^{13}C NMR (100 MHz, CDCl$_3$, 25 °C, TMS): δ = 30.2 (CH*C*H$_2$COOH), 52.4 (NH*C*HCOOH), 81.4 (≡*C*H), 82.3 (≡*C*-), 125.7, 127.1, 132.0, 132.2, 132.5, 133.4 (Ar), 166.3 (*C*ONH), 172.3 (CH*C*OOH), 173.7 (CHCH$_2$*C*OOH).

Monomer 3: Synthesized from **3′** and 4-hydroxy-TEMPO in a manner similar to **2**. The product was obtained as an orange-red solid in 80 % yield. M.p. 137.0–139.0 °C; IR (KBr): $\tilde{v}$ = 3243 (H-C≡), 2974, 2927, 2102 (C≡C), 1712 (C=O), 1604, 1562, 1465, 1365, 1307, 1268 (C-O), 1173, 1 103, 971, 906, 856, 763, 663, 556 cm^{-1}; elemental analysis calcd (%) for C$_{54}$H$_{80}$O$_{14}$N$_6$: C 62.53, H 7. 77, N 8.10; found: C 62.30, H 7.59, N 8.30.

Monomer 4: Synthesized from N-(4-ethynyl benzoyl)-L-aspartic acid, which was prepared form N-(4-ethynyl benzoyl)-L-aspartic acid methyl ester and 4-hydroxy-TEMPO in a manner similar to **3**. The product was obtained as an orange-red solid in 80 % yield. M.p. 127.0–129.0 °C; IR (KBr): $\tilde{v}$ = 3251 (H-C≡), 2969, 2889, 2105 (C≡C), 1731 (C=O), 1604, 1562, 1504, 1465, 1403, 1373, 1365, 1292 (C-O), 1200, 1164, 1084, 987, 856, 759, 674, 578 cm^{-1}; elemental analysis calcd (%) for C$_{31}$H$_{43}$O$_7$N$_3$: C 65.36, H 7.61, N 7.38; found: C 65.50, H 7.59, N 7.50.

4-Ethynylbenzoic acid 4-(2,2,6,6-tetramethyl-1-piperidinyloxy) ester (5): Prepared in a manner similar to **1**. The product was obtained as an orange-red solid in 82 % yield. M.p. 121.0–123.0 °C; IR (KBr): $\tilde{v}$ = 3243

(H-C≡), 2974, 2931, 2102 (C≡C), 1712 (C=O), 1604, 1455, 1365, 1307, 1268, 1238, 1194, 1168 (C-O), 1106, 971, 856, 767, 686, 648 cm^{-1}; elemental analysis calcd (%) for $C_{18}H_{22}NO_3$: C 71.97, H 7.38, N 4.66; found: C 72.01, H 7.32, N 4.61.

1-Pentyne-4,4-dimethyl di(2,2,5,5-tetramethyl-1-piperidinyloxyl-carboxylate) (6): Synthesized from 1-pentyne-4,4-dimethanol and 4-carboxy-TEMPO (2 equiv) in a manner similar to **1**. The product was obtained as an orange-red solid in 32% yield. M.p. 112.0–113.0°C; IR (KBr): $\tilde{v}=$ 3433, 3314, 2972, 2931, 2120, 1725 (C=O), 1473, 1376, 1364 (N−O), 1292, 1243, 1167, 1040, 973, 871, 747, 647, 632 cm^{-1}; elemental analysis calcd (%) for $C_{27}H_{44}N_2O_6$: C 65.83, H 9.00, N 5.69; found: C 65.62, H 8.67, N 5.57.

Polymerization procedures: The polymerization of monomers **1–8** was carried out with [Rh$^+$(nbd){η^6-C$_6$H$_5$B$^-$(C$_6$H$_5$)$_3$}] as the catalyst in dry solvents at 30°C for 24 h. After polymerization, the resultant solutions were poured into a large amount of methanol to precipitate the formed polymers, which were filtered and dried under reduced pressure.

IR (KBr) data of the polymers: Poly(**1**): $\tilde{v}=$ 3460, 2974, 2945, 1733, 1458, 1363, 1310, 1168, 968, 649 cm^{-1}; poly(**2**): $\tilde{v}=$ 3456, 2976, 2937, 1718, 1364, 1288, 1240, 1131, 1067, 970, 732, 645 cm^{-1}; poly(**3**): $\tilde{v}=$ 3478, 2978, 2937, 1724, 1605, 1515, 1434, 1380, 1364, 1257, 1162, 1110, 1049, 910, 852, 744 cm^{-1}; poly(**4**): $\tilde{v}=$ 3444, 2977, 2935, 1735, 1646, 1600, 1515, 1461, 1373, 1364, 1303, 1253, 1191, 1149, 1064, 995, 856, 671 cm^{-1}; poly(**5**): $\tilde{v}=$ 3444, 2973, 2897, 1716, 1605, 1562, 1465, 1364, 1311, 1272, 1176, 1106, 1014, 802, 763, 482 cm^{-1}; poly(**6**): $\tilde{v}=$ 3464, 2974, 2938, 1734, 1459, 1377, 1364, 1306, 1242, 1193, 1164, 1104, 1018, 971, 722, 648 cm^{-1}; poly(**7**): $\tilde{v}=$ 3469, 2978, 2937, 1734, 1458, 1364, 1308, 1240, 1162, 964 cm^{-1}; poly(**8**): $\tilde{v}=$ 3450, 3054, 3016, 2954, 2897, 1596, 1494, 1440, 1364, 1248, 1118, 856, 833, 689, 553 cm^{-1}.

Fabrication and electrochemical measurements of the batteries using the polymers: A coin-type cell was fabricated by stacking electrodes (1.13 cm^2) with porous polyolefin separator films. A cathode was formed by pressing the composites of a polymer (10 wt%), carbon fiber (80 wt%), and fluorinated polyolefin binder (10 wt%) as described in a previous report.[25] The cathode was set to a coin-type cell with a lithium-metal anode. A composite solution of ethylene carbonate/diethyl carbonate (30:70 v/v) containing LiPF$_6$ (1 M) was used as the electrolyte. The charge/discharge properties were measured at 25°C using a computer-controlled automatic battery charge and discharge instrument (Keisoku-kiki, Co. Ltd., Battery Labo System BLS5500).

Theoretical capacity of polymer-based cell: The theoretical capacity (Ah kg^{-1}) of an electroactive polymer was calculated from the molecular weight required per exchangeable unit charge in a polymer [Eq. (1)]:[26]

$$C(\mathrm{A\,h\,kg^{-1}}) = \frac{N_A \cdot e}{3600 \cdot (M_w/1000)} \qquad (1)$$

where $N_A \times e$ is the Faraday constant (96 487 C mol^{-1}), while M_w is the equivalent weight (or mass) of polymer in g and is defined as the molecular weight (molar mass) of the repeating unit of polymer divided by the number of electrons exchanged or stored by it (which may be a fractional number) or as the molecular weight of the set of repeating units exchanging (storing) one electron in polymers.

Acknowledgements

[1] a) C. G. Martinez, S. Jockusch, M. Ruzzi, E. Sartori, A. Moscatelli, N. J. Turro, A. L Buchachenko, *J. Phys. Chem. A* **2005**, *109*, 10216–

10221; b) K. Matsuda, M. T. Stone, J. S. Moore, *J. Am. Chem. Soc.* **2002**, *124*, 11836–11837.

[2] a) C. J. Hawker, A. W. Bosman, E. Harth, *Chem. Rev.* **2001**, *101*, 3661–3688; b) A. L. J. Beckwith, V. W. Bowry, K. U. Ingold, *J. Am. Chem. Soc.* **1992**, *114*, 4983–4992.

[3] a) I. Streeter, A. J. Wain, M. Thompson, R. G. Compton, *J. Phys. Chem. A* **2005**, *109*, 12636–12649; b) O. W. Maender, J. G. Edward, *J. Org. Chem.* **1969**, *34*, 4072–4082; c) H. Griffith, J. F. W. Keana, S. Rottschaefer, T. A. Warlick, *J. Am. Chem. Soc.* **1967**, *89*, 5072–5072.

[4] a) Y. Miwa, K. Yamamoto, M. Sakaguchi, M. Sakai, K. Tanida, S. Hara, S. Okamoto, S. Shimada, *Macromolecules* **2004**, *37*, 831–839; b) Z. Veksli, W. G. Miller, *Macromolecules* **1977**, *10*, 686–692.

[5] a) T. Iwamoto, H. Masuda, S. Ishida, C. Kabuto, M. Kira, *J. Am. Chem. Soc.* **2003**, *125*, 9300–9301; b) A. Petr, L. Dunsch, D. Koradecki, W. Kutner, *J. Electroanal. Chem.* **1991**, *300*, 129–146.

[6] a) C. D. Anderson, K. J. Shea, S. D. Rychnovsky, *Org. Lett.* **2005**, *7*, 4879–4882; b) P. Ferreira, E. Phillips, D. Rippon, S. C. Tsang, W. Hayes, *J. Org. Chem.* **2004**, *69*, 6851–6859; c) C. Tanyeli, A. Gümüş, *Tetrahedron Lett.* **2003**, *44*, 1639–1642; d) F. MacCorquodale, J. A. Crayston, J. C. Walton, D. J. Worsfold, *Tetrahedron Lett.* **1990**, *31*, 771–774.

[7] a) H. Nishide, *Adv. Mater.* **1995**, *7*, 937–941; b) A. Rajca, *Chem. Rev.* **1994**, *94*, 871–893; c) H. Iwamura, N. Koga, *Acc. Chem. Res.* **1993**, *26*, 346–351; d) A. Fujii, T. Ishida, N. Koga, H. Iwamura, *Macromolecules* **1991**, *24*, 1077–1082.

[8] a) T. L. Makarova, F. Palacio, *Carbon-Based Magnetism*, Elsevier, Amsterdam, **2006**; b) J. S. Miller, M. Drillon, *Magnetism: Molecules to Materials III*, Wiley-VCH, Weinheim, **2002**; c) K. Itoh, M. Kinoshita, *Molecular Magnetism: New Magnetic Materials*, Kohdansha and Gordon & Breach, Tokyo, **2000**.

[9] a) H. Murata, D. Miyajima, H. Nishide, *Macromolecules* **2006**, *39*, 6331–6335; b) T. Itoh, Y. Jinbo, K. Hirai, H. Tomioka, *J. Am. Chem. Soc.* **2005**, *127*, 1650–1651; c) H. Murata, D. Miyajima, R. Takada, H. Nishide, *Polym. J.* **2005**, *37*, 818–825; d) O. Nagao, M. Kozaki, Y. Miura, D. Shiomi, K. Sato, T. Takui, K. Okada, *Synth. Met.* **2003**, *105*, 95–96; e) H. Nishide, M. Nambo, M. Miyasaka, *J. Mater. Chem.* **2002**, *12*, 3578–3584; f) H. Nishide, T. Ozawa, M. Miyasaka, E. Tsuchida, *J. Am. Chem. Soc.* **2001**, *123*, 5942–5946; g) H. Oka, T. Tamura, Y. Miura, Y. Teki, *J. Mater. Chem.* **2001**, *11*, 1364–1369; h) H. Nishide, M. Miyasaka, E. Tsuchida, *J. Org. Chem.* **1998**, *63*, 7399–7407.

[10] a) R. A. Sheldon, I. W. C. E. Arends, G. J. T. Brink, A. Dijksman, *Acc. Chem. Res.* **2002**, *35*, 774–781; b) J. F. W. Keana, *Chem. Rev.* **1978**, *78*, 37–64.

[11] a) L. Columbus, W. L. Hubbell, *Trends Biochem. Sci.* **2002**, *27*, 288–295; b) M. F. Ottaviani, K. Cossu, N. J. Turro, *J. Am. Chem. Soc.* **1995**, *117*, 4387–4398; c) D. A. Middleton, D. G. Reid, A. Watts, *Biochemistry* **1995**, *34*, 7420–7429; d) M. Essman, K. Hideg, D. Marsh, *Biochemistry* **1994**, *33*, 3693–3697.

[12] V. W. Bowry, K. U. Ingold, *J. Am. Chem. Soc.* **1992**, *114*, 4992–4996.

[13] a) W. Adam, C. R. Saha-Möller, P. A. Ganeshpure, *Chem. Rev.* **2001**, *101*, 3499–3548; b) J. S. Arterburn, *Tetrahedron* **2001**, *57*, 9765–9768.

[14] a) M. Satoh, K. Nakahara, J. Iriyama, S. Iwasa, M. Suguro, *Rev. Int. Criminol. Police Tech. IEICE Trans. Electron.* **2004**, E87-C, 2076; b) H. Nishide, S. Iwasa, Y. J. Pu, T. Suga, K. Nakahara, M. Satoh, *Electrochim. Acta* **2004**, *50*, 827–831; c) K. Nakahara, S. Iwasa, M. Satoh, Y. Morioka, J. Iriyama, M. Suguro, E. Hasegawa, *Chem. Phys. Lett.* **2002**, *359*, 351–354.

[15] a) H. Nishide, T. Suga, *Electrochem. Soc. Interface* **2005**, *14*, 32–36; b) H. Nishide, S. Iwasa, Y. J. Pu, T. Suga, K. Nakahara, M. Satoh, *Electrochim. Acta* **2004**, *50*, 827–831; c) K. Nakahara, S. Iwasa, M. Satoh, Y. Morioka, J. Iriyama, M. Suguro, E. Hasegawa, *Chem. Phys. Lett.* **2002**, *359*, 351–354.

[16] a) M. Satoh, K. Nakahara, J. Iriyama, S. Iwasa, M. Suguro, *Rev. Int. Criminol. Police Tech. IEICE Trans. Electron.* **2004**, E87-C, 2076; b) H. Nishide, S. Iwasa, Y. J. Pu, T. Suga, K. Nakahara, M. Satoh, *Electrochim. Acta* **2004**, *50*, 827–831; c) K. Nakahara, S. Iwasa, M.

Satoh, Y. Morioka, J. Iriyama, M. Suguro, E. Hasegawa, *Chem. Phys. Lett.* **2002**, *359*, 351–354.

[17] T. Katsumata, M. Satoh, J. Wada, M. Shiotsuki, F. Sanda, T. Masuda, *Macromol. Rapid Commun.* **2006**, *27*, 1206–1211.

[18] T. Suga, Y. J. Pu, S. Kasatori, H. Nishide, *Macromolecules*, **2007**, *40*, 3167–3173.

[19] a) T. Masuda, *J. Polym. Sci Part A: Polym Chem.* **2007**, *45*, 165–180; b) J. W. Y. Lam, B. Z. Tang, *Acc. Chem. Res.* **2005**, *38*, 745–754; c) E. Yashima, K. Maeda, T. Nishimura, *Chem. Eur. J.* **2004**, *10*, 42–51; d) T. Masuda, F. Sanda, in *Handbook of Metathesis, Vol. 3* (Ed.: R. H. Grubbs), Wiley-VCH, Weinheim, **2003**, Chapter 3; e) K. Nagai, T. Masuda, T. Nakagawa, B. D. Freeman, I. Pinnau, *Prog. Polym. Sci.* **2001**, *26*, 721–798.

[20] R. A. Findeis, L. H. Gade, *J. Chem. Soc. Dalton Trans.* **2002**, 3952–3960.

[21] E. Yashima, T. Matsushima, Y. Okamoto, *J. Am. Chem. Soc.* **1997**, *119*, 6345–6359.

[22] a) K. L. Cheuk, B. Z. Tang, *ACS Symp. Ser.* **2005**, *888*, 340–358; b) K. K. L. Cheuk, J. W. Y. Lam, J. Chen, L. M. Lai, B. Z. Tang, *Macromolecules* **2003**, *36*, 5947–5959.

[23] R. R. Schrock, J. A. Osborn, *Inorg. Chem.* **1970**, *9*, 2339–2343.

[24] K. Mizoguchi, *Jpn. J. Appl.* **1995**, 34, 1–19.

[25] J. Qu, T. Katsumata, M. Satoh, J. Wada, T. Masuda, *Macromolecule* **2007**, *40*, 3136–3144.

[26] P. Passiniemi, J. E. Österholm, *Synth. Met.* **1987**, *18*, 637–644.